

Accelerating PDE-Constrained Optimization Problems using Adaptive Reduced-Order Models

Matthew J. Zahr

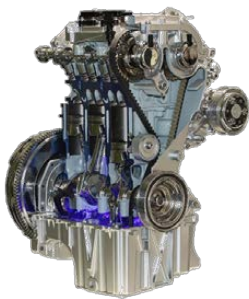
Advisor: Charbel Farhat
Computational and Mathematical Engineering
Stanford University

Argonne National Laboratory, Argonne, IL
January 15, 2016



Multiphysics Optimization Key Player in Next-Gen Problems

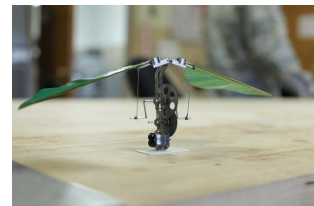
*Current interest in computational physics reaches far beyond analysis of a single configuration of a physical system into **design** (shape and topology¹), **control**, and **uncertainty quantification***



Engine System



EM Launcher



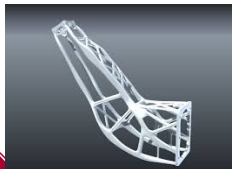
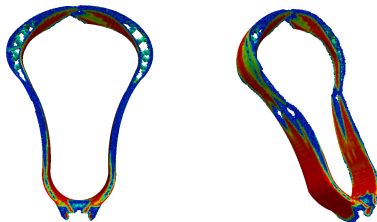
Micro-Aerial Vehicle



¹Emergence of additive manufacturing technologies has made topology optimization increasingly relevant, particularly in DOE.

Topology Optimization and Additive Manufacturing²

- Emergence of AM has made TO an increasingly relevant topic
- AM+TO lead to highly efficient designs that could not be realized previously
- Challenges: smooth topologies require **very fine** meshes and modeling of complex **manufacturing process**



²MIT Technology Review, Top 10 Technological Breakthrough 2013

PDE-Constrained Optimization I

Goal: Rapidly solve PDE-constrained optimization problem of the form

$$\begin{aligned} & \underset{\boldsymbol{u} \in \mathbb{R}^{n_u}, \boldsymbol{\mu} \in \mathbb{R}^{n_\mu}}{\text{minimize}} && \mathcal{J}(\boldsymbol{u}, \boldsymbol{\mu}) \\ & \text{subject to} && \boldsymbol{r}(\boldsymbol{u}, \boldsymbol{\mu}) = 0 \end{aligned}$$

where

- $\boldsymbol{r} : \mathbb{R}^{n_u} \times \mathbb{R}^{n_\mu} \rightarrow \mathbb{R}^{n_u}$ is the discretized partial differential equation
- $\mathcal{J} : \mathbb{R}^{n_u} \times \mathbb{R}^{n_\mu} \rightarrow \mathbb{R}$ is the objective function
- $\boldsymbol{u} \in \mathbb{R}^{n_u}$ is the PDE state vector
- $\boldsymbol{\mu} \in \mathbb{R}^{n_\mu}$ is the vector of parameters

red indicates a large-scale quantity, $\mathcal{O}(\text{mesh})$



Nested Approach to PDE-Constrained Optimization

Virtually all expense emanates from primal/dual PDE solvers

Optimizer

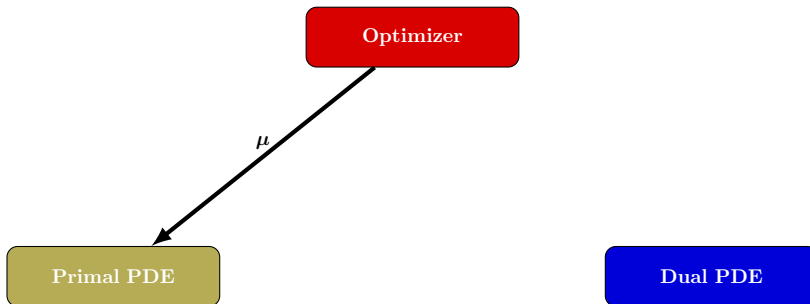
Primal PDE

Dual PDE



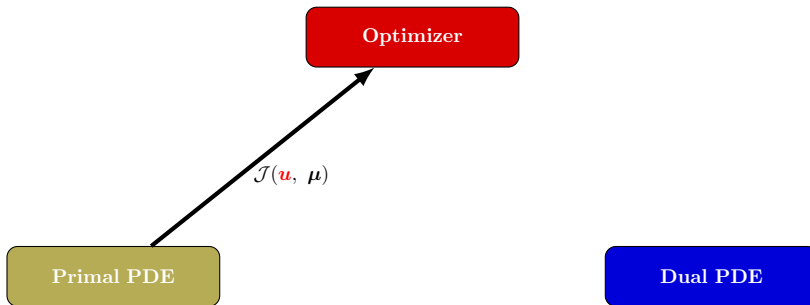
Nested Approach to PDE-Constrained Optimization

Virtually all expense emanates from primal/dual PDE solvers



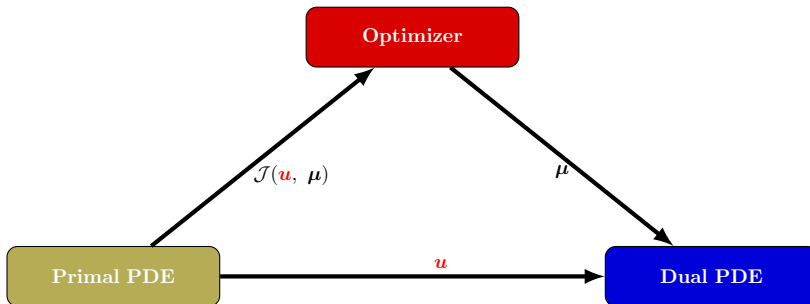
Nested Approach to PDE-Constrained Optimization

Virtually all expense emanates from primal/dual PDE solvers



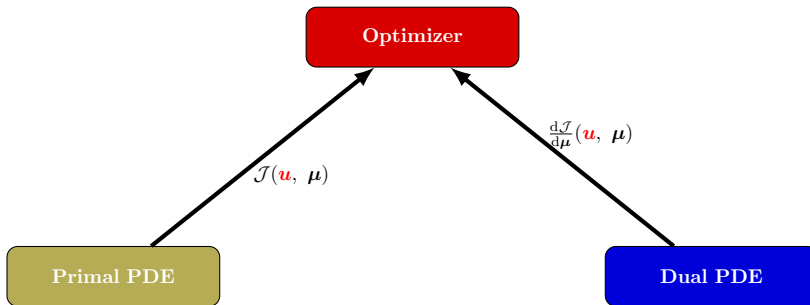
Nested Approach to PDE-Constrained Optimization

Virtually all expense emanates from primal/dual PDE solvers



Nested Approach to PDE-Constrained Optimization

Virtually all expense emanates from primal/dual PDE solvers



Projection-Based Model Reduction to Reduce PDE Size

- Model Order Reduction (MOR) assumption: *state vector lies in low-dimensional subspace*

$$\mathbf{u} \approx \Phi_{\mathbf{u}} \mathbf{u}_r \quad \frac{\partial \mathbf{u}}{\partial \boldsymbol{\mu}} \approx \Phi_{\mathbf{u}} \frac{\partial \mathbf{u}_r}{\partial \boldsymbol{\mu}}$$

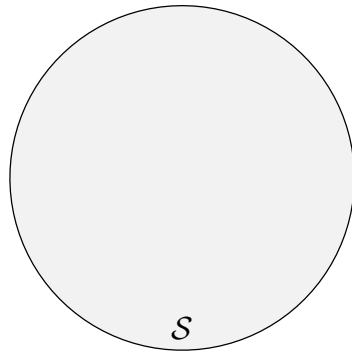
where

- $\Phi_{\mathbf{u}} = [\phi_{\mathbf{u}}^1 \quad \dots \quad \phi_{\mathbf{u}}^{k_{\mathbf{u}}}] \in \mathbb{R}^{n_{\mathbf{u}} \times k_{\mathbf{u}}}$ is the reduced basis
- $\mathbf{u}_r \in \mathbb{R}^{k_{\mathbf{u}}}$ are the reduced coordinates of \mathbf{u}
- $n_{\mathbf{u}} \gg k_{\mathbf{u}}$
- Substitute assumption into High-Dimensional Model (HDM), $\mathbf{r}(\mathbf{u}, \boldsymbol{\mu}) = 0$, and project onto test subspace $\Psi_{\mathbf{u}} \in \mathbb{R}^{n_{\mathbf{u}} \times k_{\mathbf{u}}}$

$$\Psi_{\mathbf{u}}^T \mathbf{r}(\Phi_{\mathbf{u}} \mathbf{u}_r, \boldsymbol{\mu}) = 0$$



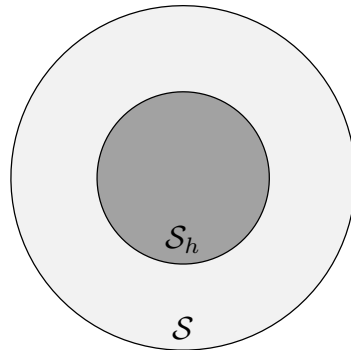
Connection to Finite Element Method: Hierarchical Subspaces



- \mathcal{S} - infinite-dimensional trial space



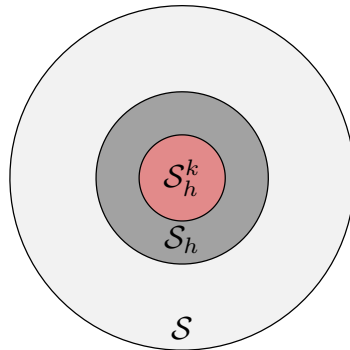
Connection to Finite Element Method: Hierarchical Subspaces



- \mathcal{S} - infinite-dimensional trial space
- \mathcal{S}_h - (large) finite-dimensional trial space



Connection to Finite Element Method: Hierarchical Subspaces



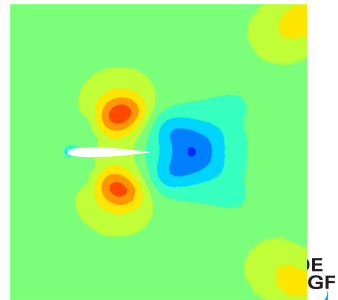
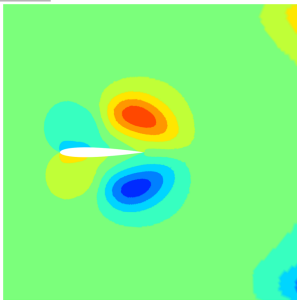
- \mathcal{S} - infinite-dimensional trial space
- \mathcal{S}_h - (large) finite-dimensional trial space
- \mathcal{S}_h^k - (small) finite-dimensional trial space
- $\mathcal{S}_h^k \subset \mathcal{S}_h \subset \mathcal{S}$



Few Global, Data-Driven Basis Functions v. Many Local Ones



- Instead of using traditional *local* shape functions (e.g., FEM), use *global* shape functions
- Instead of a-priori, analytical shape functions, leverage data-rich computing environment by using *data-driven* modes



Definition of Φ_u : Data-Driven Reduction

State-Sensitivity Proper Orthogonal Decomposition (POD)

- Collect state and sensitivity snapshots by sampling HDM

$$\mathbf{X} = [\mathbf{u}(\boldsymbol{\mu}_1) \quad \mathbf{u}(\boldsymbol{\mu}_2) \quad \cdots \quad \mathbf{u}(\boldsymbol{\mu}_n)]$$

$$\mathbf{Y} = \left[\frac{\partial \mathbf{u}}{\partial \boldsymbol{\mu}}(\boldsymbol{\mu}_1) \quad \frac{\partial \mathbf{u}}{\partial \boldsymbol{\mu}}(\boldsymbol{\mu}_2) \quad \cdots \quad \frac{\partial \mathbf{u}}{\partial \boldsymbol{\mu}}(\boldsymbol{\mu}_n) \right]$$

- Use Proper Orthogonal Decomposition to generate reduced basis for each individually

$$\Phi_{\mathbf{X}} = \text{POD}(\mathbf{X})$$

$$\Phi_{\mathbf{Y}} = \text{POD}(\mathbf{Y})$$

- Concatenate to get reduced-order basis

$$\Phi_u = [\Phi_{\mathbf{X}} \quad \Phi_{\mathbf{Y}}]$$



Definition of Ψ_u : Minimum-Residual ROM

Least-Squares Petrov-Galerkin (LSPG)³ projection

$$\Psi_u = \frac{\partial \mathbf{r}}{\partial \mathbf{u}} \Phi_u$$

Minimum-Residual Property

A ROM possesses the minimum-residual property if $\Psi_u \mathbf{r}(\Phi_u \mathbf{u}_r, \mu) = 0$ is equivalent to the optimality condition of $(\Theta \succ 0)$

$$\underset{\mathbf{u}_r \in \mathbb{R}^{k_u}}{\text{minimize}} \quad \|\mathbf{r}(\Phi_u \mathbf{u}_r, \mu)\|_{\Theta}$$

- Implications
 - Recover exact solution when basis not truncated (consistent³)
 - Monotonic improvement of solution as basis size increases
 - Ensures sensitivity information in Φ cannot degrade state approximation⁴
- LSPG possesses minimum-residual property



³[Bui-Thanh et al., 2008]

⁴[Fahl, 2001]



Definition of $\frac{\partial \mathbf{u}_r}{\partial \boldsymbol{\mu}}$: Minimum-Residual Reduced Sensitivities

Traditional sensitivity analysis

$$\frac{\partial \mathbf{u}_r}{\partial \boldsymbol{\mu}} = - \left[\sum_{j=1}^N \mathbf{r}_j \Phi_{\mathbf{u}}^T \frac{\partial \mathbf{r}_j}{\partial \mathbf{u} \partial \boldsymbol{\mu}} \Phi_{\mathbf{u}} + \left(\frac{\partial \mathbf{r}}{\partial \mathbf{u}} \Phi_{\mathbf{u}} \right)^T \frac{\partial \mathbf{r}}{\partial \mathbf{u}} \Phi_{\mathbf{u}} \right]^{-1} \\ \left(\sum_{j=1}^N \mathbf{r}_j \Phi_{\mathbf{u}}^T \frac{\partial^2 \mathbf{r}_j}{\partial \mathbf{u} \partial \boldsymbol{\mu}} + \left(\frac{\partial \mathbf{r}}{\partial \mathbf{u}} \Phi_{\mathbf{u}} \right)^T \frac{\partial \mathbf{r}}{\partial \boldsymbol{\mu}} \right)$$

- + Guaranteed to give rise to *exact* derivatives of ROM quantities of interest
 - Requires 2nd derivatives of \mathbf{r}
 - $\Phi_{\mathbf{u}} \frac{\partial \mathbf{u}_r}{\partial \mathbf{u}}$ not guaranteed to be good approximate to full sensitivity $\frac{\partial \mathbf{u}}{\partial \mathbf{u}}$



Definition of $\frac{\partial \widehat{\mathbf{u}}_r}{\partial \boldsymbol{\mu}}$: Minimum-Residual Reduced Sensitivities

Minimum-residual sensitivity analysis

$$\widehat{\frac{\partial \mathbf{u}_r}{\partial \boldsymbol{\mu}}} = \arg \min_{\mathbf{a}} \|\Phi_{\mathbf{u}} \mathbf{a} - \frac{\partial \mathbf{u}}{\partial \boldsymbol{\mu}}\|_{\Theta} = - \left[\left(\frac{\partial \mathbf{r}}{\partial \mathbf{u}} \Phi_{\mathbf{u}} \right)^T \frac{\partial \mathbf{r}}{\partial \mathbf{u}} \Phi_{\mathbf{u}} \right]^{-1} \left(\frac{\partial \mathbf{r}}{\partial \mathbf{u}} \Phi_{\mathbf{u}} \right)^T \frac{\partial \mathbf{r}}{\partial \boldsymbol{\mu}}$$

- + Minimum-residual property - $\Phi_{\mathbf{u}} \frac{\widehat{\partial \mathbf{u}_r}}{\partial \boldsymbol{\mu}}$ is Θ -optimal solution to $\frac{\partial \mathbf{u}}{\partial \boldsymbol{\mu}}$ in $\Phi_{\mathbf{u}}$
- + Does not require 2nd derivatives of \mathbf{r}
- $\widehat{\frac{\partial \mathbf{u}_r}{\partial \boldsymbol{\mu}}} \neq \frac{\partial \mathbf{u}_r}{\partial \boldsymbol{\mu}}$, i.e., it is not the true ROM sensitivity



Offline-Online Approach to Optimization



Schematic



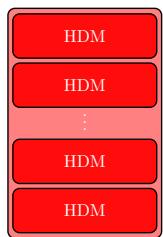
μ -space



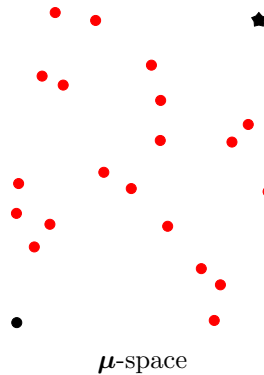
Breakdown of Computational Effort



Offline-Online Approach to Optimization



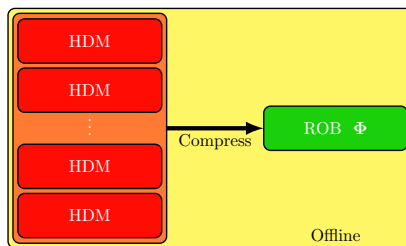
Schematic



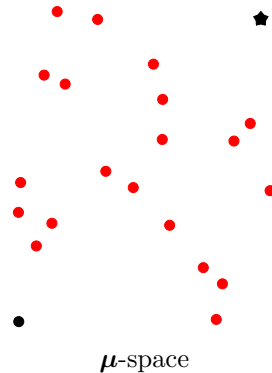
Breakdown of Computational Effort



Offline-Online Approach to Optimization



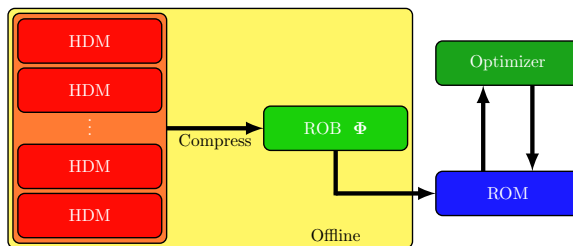
Schematic



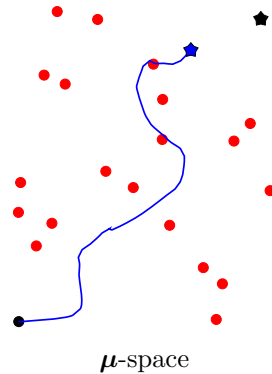
Breakdown of Computational Effort



Offline-Online Approach to Optimization



Schematic

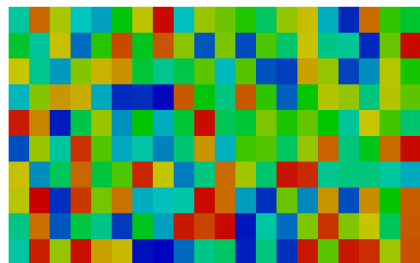


Breakdown of Computational Effort



Numerical Demonstration: Offline-Online Breakdown

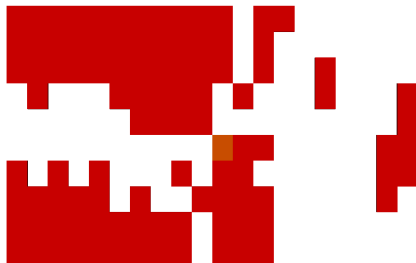
- Parameter reduction (Φ_{μ})
 - *apriori spatial clustering*
 - $k_{\mu} = 200$
- *Greedy* Training
 - 5000 candidate points (LHS)
 - 50 snapshots
 - Error indicator: $\|\mathbf{r}(\Phi_{\mathbf{u}} \mathbf{u}_r, \Phi_{\mu} \boldsymbol{\mu}_r)\|$
- State reduction ($\Phi_{\mathbf{u}}$)
 - POD
 - $k_{\mathbf{u}} = 25$
 - Polynomialization acceleration



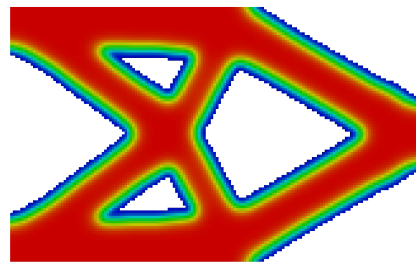
Material Basis



Numerical Demonstration: Offline-Online Breakdown



Optimal Solution (ROM)



Optimal Solution (HDM)

HDM Solution	ROB Construction	Greedy Algorithm	ROM Optimization
2.84×10^3 s	5.48×10^4 s	1.67×10^5 s	30 s
1.26%	24.36%	74.37%	0.01%



HDM Optimization: 1.97×10^4 s



ROM-Based Trust-Region Framework for Optimization



Schematic



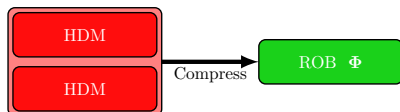
μ -space



Breakdown of Computational Effort



ROM-Based Trust-Region Framework for Optimization



Schematic



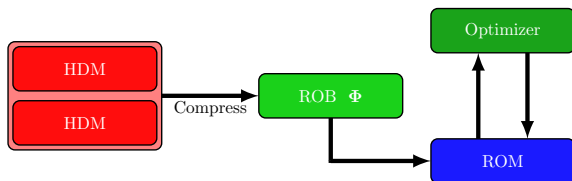
μ -space



Breakdown of Computational Effort



ROM-Based Trust-Region Framework for Optimization



Schematic



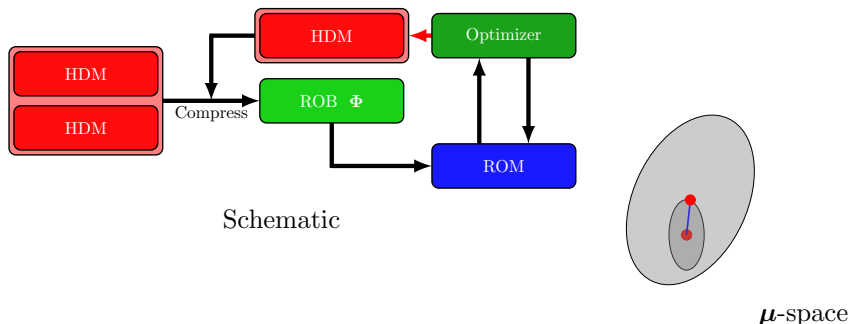
μ -space



Breakdown of Computational Effort



ROM-Based Trust-Region Framework for Optimization



Schematic

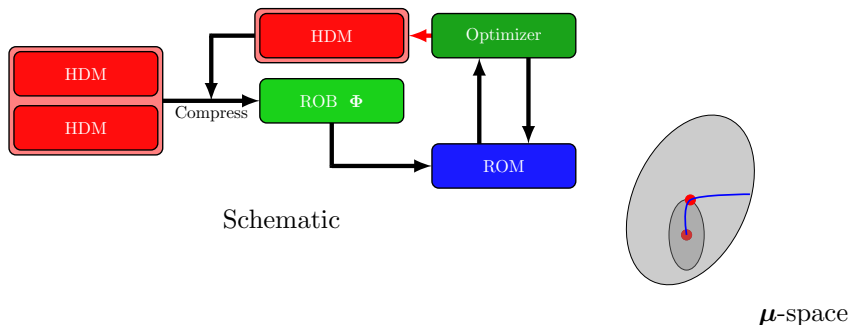
μ -space



Breakdown of Computational Effort



ROM-Based Trust-Region Framework for Optimization



Schematic

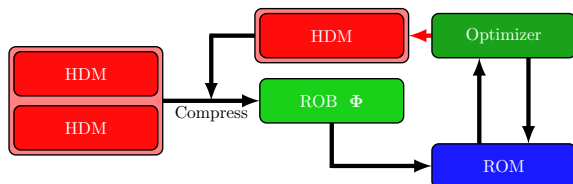
μ -space



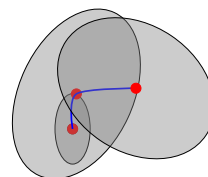
Breakdown of Computational Effort



ROM-Based Trust-Region Framework for Optimization



Schematic



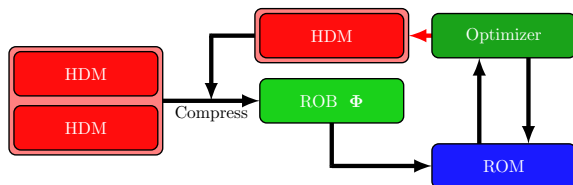
μ -space



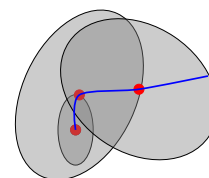
Breakdown of Computational Effort



ROM-Based Trust-Region Framework for Optimization



Schematic



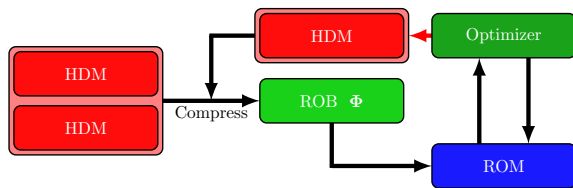
μ -space



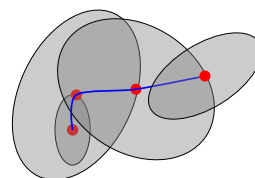
Breakdown of Computational Effort



ROM-Based Trust-Region Framework for Optimization



Schematic



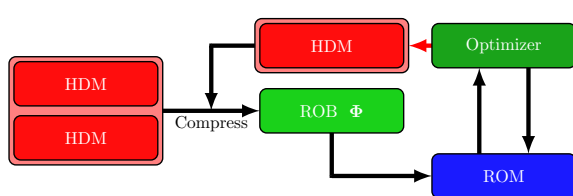
μ -space



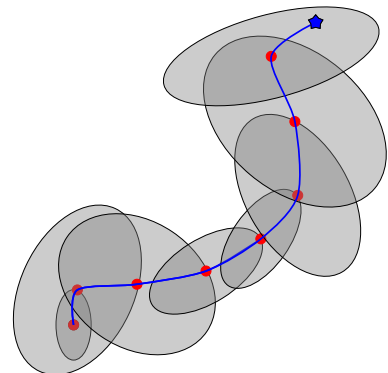
Breakdown of Computational Effort



ROM-Based Trust-Region Framework for Optimization



Schematic



μ -space



Breakdown of Computational Effort



ROM-Based Trust-Region Framework for Optimization

Nonlinear Trust-Region Framework with Adaptive Model Reduction

- Collect snapshots from HDM at *sparse sampling* of the parameter space
- Build ROB $\Phi_{\mathbf{u}}$ from sparse training
- Solve optimization problem

$$\underset{\mathbf{u}_r \in \mathbb{R}^{k_u}, \mu \in \mathbb{R}^{n_\mu}}{\text{minimize}} \quad \mathcal{J}(\Phi_{\mathbf{u}} \mathbf{u}_r, \mu)$$

$$\text{subject to} \quad \Phi_{\mathbf{u}}^T \mathbf{r}(\Phi_{\mathbf{u}} \mathbf{u}_r, \mu) = 0$$

$$\|\mathbf{r}(\Phi_{\mathbf{u}} \mathbf{u}_r, \mu)\| \leq \Delta$$

- Use solution of above problem to enrich training, adapt Δ using standard trust-region methods, and repeat until convergence

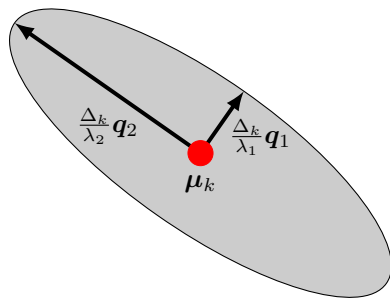


Residual-Based Trust-Region Interpretation

Let $\hat{\mathbf{r}}(\boldsymbol{\mu}) = \mathbf{r}(\Phi_{\mathbf{u}} \mathbf{u}_r(\boldsymbol{\mu}), \boldsymbol{\mu})$ and $\mathbf{A}_k = \frac{\partial \hat{\mathbf{r}}}{\partial \boldsymbol{\mu}}(\boldsymbol{\mu}_k)^T \frac{\partial \hat{\mathbf{r}}}{\partial \boldsymbol{\mu}}(\boldsymbol{\mu}_k) = \mathbf{Q}_k \Lambda_k^2 \mathbf{Q}_k^T$.

Then, to first order⁵,

$$\|\hat{\mathbf{r}}(\boldsymbol{\mu})\|_2 = \left\| \frac{\partial \hat{\mathbf{r}}}{\partial \boldsymbol{\mu}}(\boldsymbol{\mu}_k)(\boldsymbol{\mu} - \boldsymbol{\mu}_k) \right\|_2 = \|\boldsymbol{\mu} - \boldsymbol{\mu}_k\|_{\mathbf{A}_k} \leq \Delta_k$$



Annotated schematic of trust-region: $\mathbf{q}_i = \mathbf{Q}_k \mathbf{e}_i$ and $\lambda_i = \mathbf{e}_i^T \Lambda_k \mathbf{e}_i$

⁵assuming $\hat{\mathbf{r}}(\boldsymbol{\mu}_k) = 0$, i.e., ROM exact at trust-region center

ROM-Based Trust-Region Framework for Optimization

Ingredients of Proposed Approach [Zahr and Farhat, 2014]

- Minimum-residual ROM (LSPG) and minimum-error sensitivities
 - $\mathcal{J}(\mathbf{u}, \boldsymbol{\mu}) = \mathcal{J}(\Phi_{\mathbf{u}} \mathbf{u}_r, \boldsymbol{\mu})$ and $\frac{d\mathcal{J}}{d\boldsymbol{\mu}}(\mathbf{u}, \boldsymbol{\mu}) = \frac{d\mathcal{J}}{d\boldsymbol{\mu}}(\Phi_{\mathbf{u}} \mathbf{u}_r, \boldsymbol{\mu})$ for training parameters $\boldsymbol{\mu}$
- Reduced optimization (sub)problem

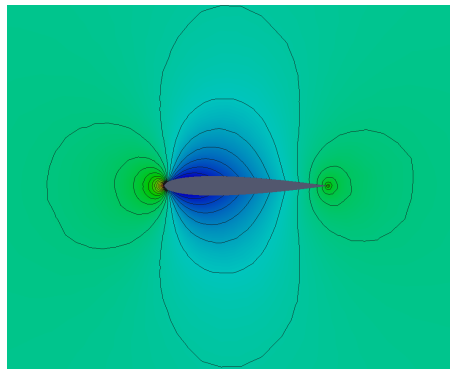
$$\begin{aligned} & \underset{\mathbf{u}_r \in \mathbb{R}^{n_{\mathbf{u}}}, \boldsymbol{\mu} \in \mathbb{R}^{n_{\boldsymbol{\mu}}}}{\text{minimize}} && \mathcal{J}(\Phi_{\mathbf{u}} \mathbf{u}_r, \boldsymbol{\mu}) \\ & \text{subject to} && \Psi_{\mathbf{u}}^T \mathbf{r}(\Phi_{\mathbf{u}} \mathbf{u}_r, \boldsymbol{\mu}) = 0 \\ & && \|\mathbf{r}(\Phi_{\mathbf{u}} \mathbf{u}_r, \boldsymbol{\mu})\|_2^2 \leq \Delta \end{aligned}$$

- Efficiently update ROB with additional snapshots or new translation vector
 - Without re-computing SVD of entire snapshot matrix
- Adaptive selection of $\Delta \rightarrow$ trust-region approach

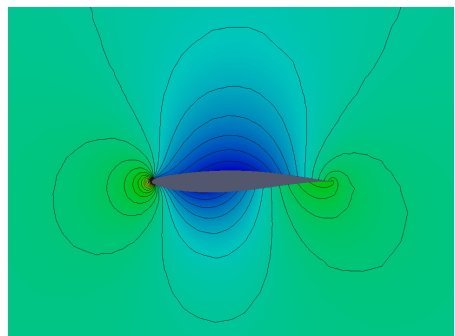


Compressible, Inviscid Airfoil Inverse Design

Pressure discrepancy minimization (Euler equations)



NACA0012: Initial

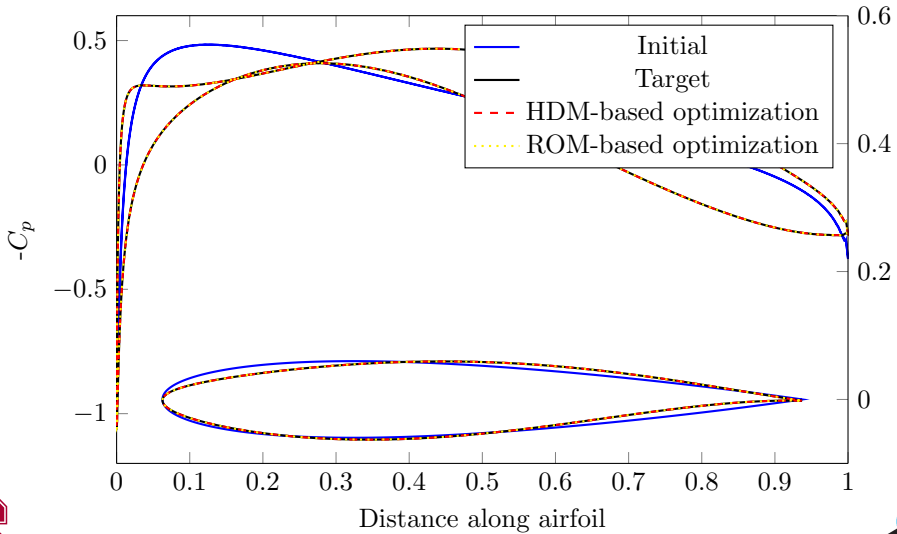


RAE2822: Target

Pressure field for airfoil configurations at $M_\infty = 0.5$, $\alpha = 0.0^\circ$



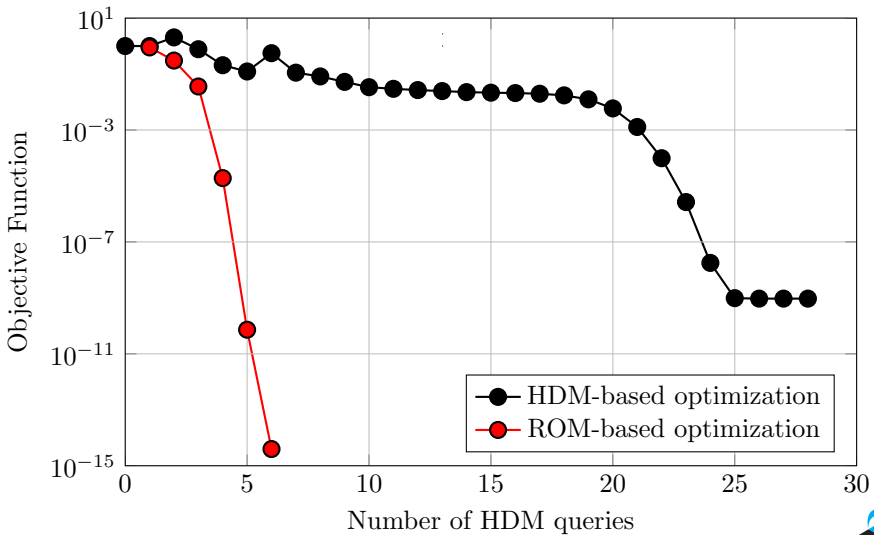
ROM-Constrained Optimization Solver Recovers Target



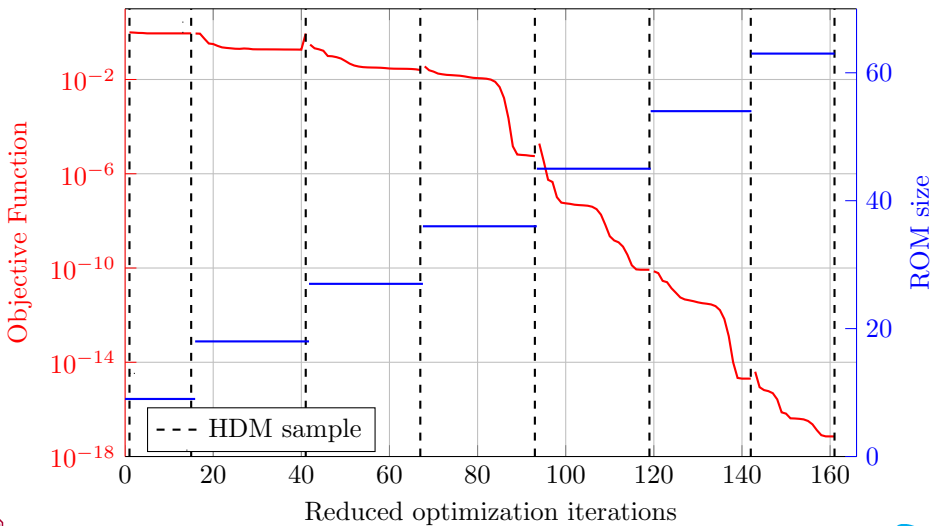
Distance Transverse to Centerline



ROM Solver Requires 4× Fewer HDM Queries

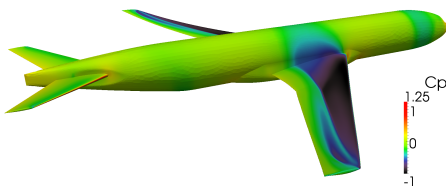


At the Cost of ROM Queries

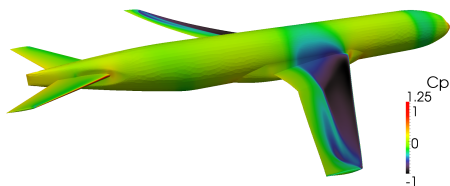


Next: Shape Optimization of Full Aircraft (CRM)

ROMs are fast, accurate, and require limited resources



HDM solution (Drag = 142.336kN)



ROM solution (Drag = 142.304kN)

- HDM: 70×10^6 DOF, **2hr on 1024** Intel Xeon E5-2698 v3 cores (2.3GHz)
- ROM: **170s on 2** Intel i7 cores (1.8GHz)
- Relative error in drag 0.022%
- CPU-time speedup greater than 2.15×10^4
- Wall-time speedup greater than **42**
- *Washabaugh, Zahr, Farhat (AIAA, 2016)*



PDE-Constrained Optimization II

Goal: Rapidly solve PDE-constrained optimization problem of the form

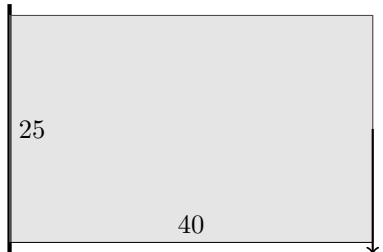
$$\begin{aligned} & \underset{\boldsymbol{u} \in \mathbb{R}^{n_u}, \boldsymbol{\mu} \in \mathbb{R}^{n_\mu}}{\text{minimize}} && \mathcal{J}(\boldsymbol{u}, \boldsymbol{\mu}) \\ & \text{subject to} && \boldsymbol{r}(\boldsymbol{u}, \boldsymbol{\mu}) = 0 \\ & && \boldsymbol{c}(\boldsymbol{u}, \boldsymbol{\mu}) \geq 0 \end{aligned}$$

where

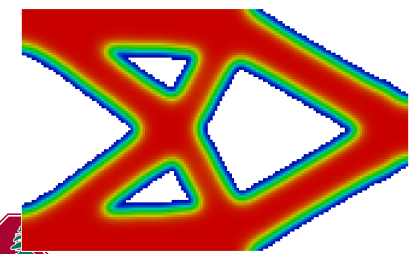
- $\boldsymbol{r} : \mathbb{R}^{n_u} \times \mathbb{R}^{n_\mu} \rightarrow \mathbb{R}^{n_u}$ is the discretized partial differential equation
- $\mathcal{J} : \mathbb{R}^{n_u} \times \mathbb{R}^{n_\mu} \rightarrow \mathbb{R}$ is the objective function
- $\boldsymbol{c} : \mathbb{R}^{n_u} \times \mathbb{R}^{n_\mu} \rightarrow \mathbb{R}^{n_c}$ are the side constraints
- $\boldsymbol{u} \in \mathbb{R}^{n_u}$ is the PDE state vector
- $\boldsymbol{\mu} \in \mathbb{R}^{n_\mu}$ is the vector of parameters



Problem Setup



- 16000 8-node brick elements, 77760 dofs
- Total Lagrangian form, finite strain, StVK⁶
- St. Venant-Kirchhoff material
- Sparse Cholesky linear solver (CHOLMOD⁷)
- Newton-Raphson nonlinear solver
- Minimum compliance optimization problem



$$\begin{aligned} & \underset{\boldsymbol{u} \in \mathbb{R}^n \boldsymbol{u}, \boldsymbol{\mu} \in \mathbb{R}^n \boldsymbol{\mu}}{\text{minimize}} && \boldsymbol{f}_{\text{ext}}^T \boldsymbol{u} \\ & \text{subject to} && V(\boldsymbol{\mu}) \leq \frac{1}{2} V_0 \\ & && \boldsymbol{r}(\boldsymbol{u}, \boldsymbol{\mu}) = 0 \end{aligned}$$

- Gradient computations: Adjoint method
- Optimizer: SNOPT [Gill et al., 2002]



⁶[Bonet and Wood, 1997, Belytschko et al., 2000]

⁷[Chen et al., 2008]



Restrict Parameter Space to Low-Dimensional Subspace

- Restrict parameter to a low-dimensional subspace

$$\boldsymbol{\mu} \approx \Phi_{\boldsymbol{\mu}} \boldsymbol{\mu}_r$$

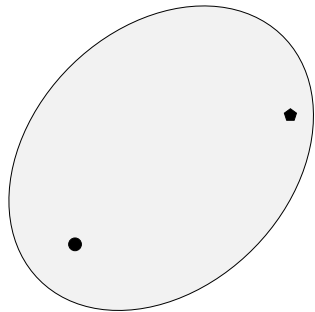
- $\Phi_{\boldsymbol{\mu}} = \begin{bmatrix} \phi_{\boldsymbol{\mu}}^1 & \dots & \phi_{\boldsymbol{\mu}}^{k_{\boldsymbol{\mu}}} \end{bmatrix} \in \mathbb{R}^{n_{\boldsymbol{\mu}} \times k_{\boldsymbol{\mu}}}$ is the reduced basis
- $\boldsymbol{\mu}_r \in \mathbb{R}^{k_{\boldsymbol{\mu}}}$ are the reduced coordinates of $\boldsymbol{\mu}$
- $n_{\boldsymbol{\mu}} \gg k_{\boldsymbol{\mu}}$
- Substitute restriction into reduced-order model to obtain

$$\Phi_{\boldsymbol{u}}^T \boldsymbol{r}(\Phi_{\boldsymbol{u}} \boldsymbol{u}_r, \Phi_{\boldsymbol{\mu}} \boldsymbol{\mu}_r) = 0$$

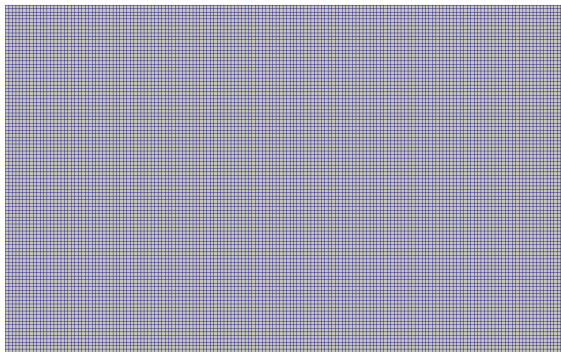
- Related work:
 [Maute and Ramm, 1995, Lieberman et al., 2010, Constantine et al., 2014]



Restrict Parameter Space to Low-Dimensional Subspace



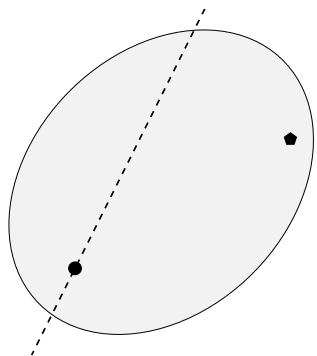
μ -space



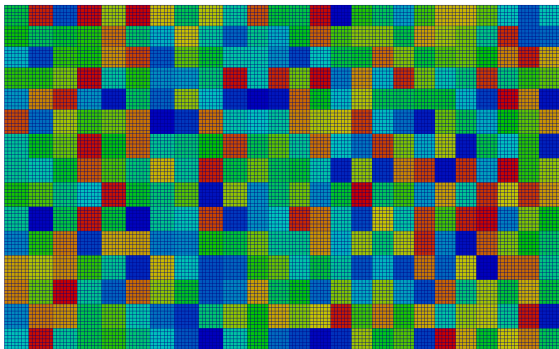
Background mesh



Restrict Parameter Space to Low-Dimensional Subspace



μ -space

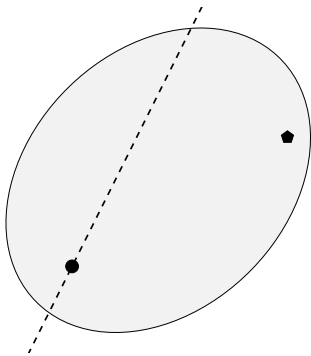


Macroelements



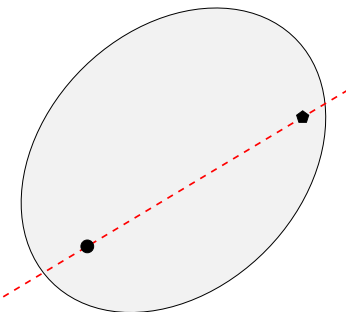
Optimality Conditions to Adapt Reduced-Order Basis, Φ_μ

- Selection of Φ_μ amounts to a *restriction* of the parameter space



Optimality Conditions to Adapt Reduced-Order Basis, Φ_μ

- Selection of Φ_μ amounts to a *restriction* of the parameter space
- Adaptation of Φ_μ should attempt to include the optimal solution in the restricted parameter space, i.e. $\mu^* \in \text{col}(\Phi_\mu)$
- Adaptation based on **first-order optimality conditions** of HDM optimization problem



Optimality Conditions to Adapt Reduced-Order Basis, Φ_μ

Lagrangian

$$\mathcal{L}(\boldsymbol{\mu}, \boldsymbol{\lambda}) = \mathcal{J}(\mathbf{u}(\boldsymbol{\mu}), \boldsymbol{\mu}) - \boldsymbol{\lambda}^T \mathbf{c}(\mathbf{u}(\boldsymbol{\mu}), \boldsymbol{\mu})$$

Karush-Kuhn Tucker (KKT) Conditions⁸

$$\nabla_{\boldsymbol{\mu}} \mathcal{L}(\boldsymbol{\mu}, \boldsymbol{\lambda}) = 0$$

$$\boldsymbol{\lambda} \geq 0$$

$$\boldsymbol{\lambda}_i \mathbf{c}_i(\mathbf{u}(\boldsymbol{\mu}), \boldsymbol{\mu}) = 0$$

$$\mathbf{c}(\mathbf{u}(\boldsymbol{\mu}), \boldsymbol{\mu}) \geq 0$$



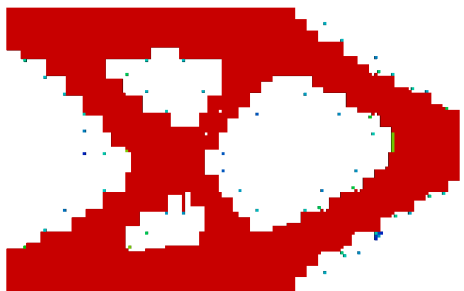
⁸[Nocedal and Wright, 2006]

Lagrangian Gradient Refinement Indicator

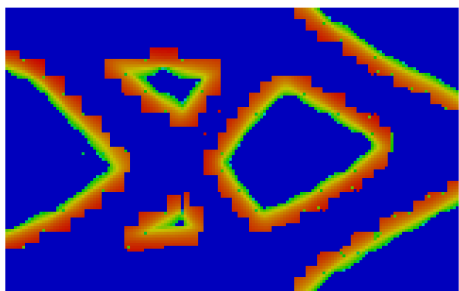
- From Lagrange multiplier estimates, only KKT condition not satisfied automatically:

$$\nabla_{\boldsymbol{\mu}} \mathcal{L}(\boldsymbol{\mu}, \boldsymbol{\lambda}) = 0$$

- Use $|\nabla_{\boldsymbol{\mu}} \mathcal{L}(\boldsymbol{\mu}, \boldsymbol{\lambda})|$ as indicator for **refinement** of discretization of $\boldsymbol{\mu}$ -space



$\boldsymbol{\mu}$



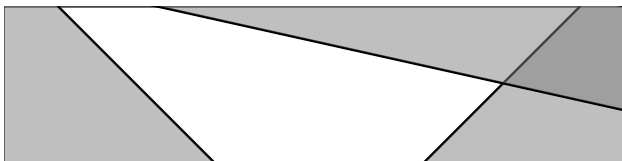
$|\nabla_{\boldsymbol{\mu}} \mathcal{L}(\boldsymbol{\mu}, \boldsymbol{\lambda})|$



Constraints may lead to infeasible sub-problems

Non-Quadratic Trust-Region MOR [Zahr and Farhat, 2014]

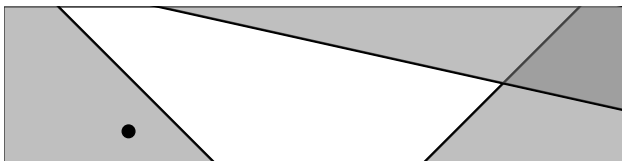
$$\begin{aligned} & \underset{\boldsymbol{u}_r \in \mathbb{R}^{k_u}, \boldsymbol{\mu}_r \in \mathbb{R}^{k_\mu}}{\text{minimize}} && \mathcal{J}(\Phi_{\boldsymbol{u}} \boldsymbol{u}_r, \Phi_{\boldsymbol{\mu}} \boldsymbol{\mu}_r) \\ & \text{subject to} && c(\Phi_{\boldsymbol{u}} \boldsymbol{u}_r, \Phi_{\boldsymbol{\mu}} \boldsymbol{\mu}_r) \geq 0 \\ & && r(\Phi_{\boldsymbol{u}} \boldsymbol{u}_r, \Phi_{\boldsymbol{\mu}} \boldsymbol{\mu}_r) = 0 \\ & && \|r(\Phi_{\boldsymbol{u}} \boldsymbol{u}_r, \Phi_{\boldsymbol{\mu}} \boldsymbol{\mu}_r)\| \leq \Delta \end{aligned}$$



Constraints may lead to infeasible sub-problems

Non-Quadratic Trust-Region MOR [Zahr and Farhat, 2014]

$$\begin{aligned} & \underset{\boldsymbol{u}_r \in \mathbb{R}^{k_u}, \boldsymbol{\mu}_r \in \mathbb{R}^{k_\mu}}{\text{minimize}} && \mathcal{J}(\Phi_{\boldsymbol{u}} \boldsymbol{u}_r, \Phi_{\boldsymbol{\mu}} \boldsymbol{\mu}_r) \\ & \text{subject to} && c(\Phi_{\boldsymbol{u}} \boldsymbol{u}_r, \Phi_{\boldsymbol{\mu}} \boldsymbol{\mu}_r) \geq 0 \\ & && r(\Phi_{\boldsymbol{u}} \boldsymbol{u}_r, \Phi_{\boldsymbol{\mu}} \boldsymbol{\mu}_r) = 0 \\ & && \|r(\Phi_{\boldsymbol{u}} \boldsymbol{u}_r, \Phi_{\boldsymbol{\mu}} \boldsymbol{\mu}_r)\| \leq \Delta \end{aligned}$$



Constraints may lead to infeasible sub-problems

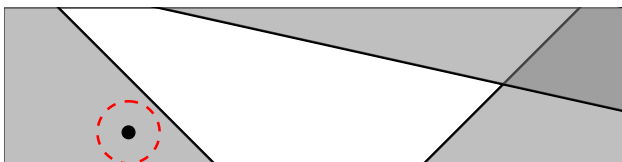
Non-Quadratic Trust-Region MOR [Zahr and Farhat, 2014]

$$\underset{\boldsymbol{u}_r \in \mathbb{R}^{k_u}, \boldsymbol{\mu}_r \in \mathbb{R}^{k_\mu}}{\text{minimize}} \quad \mathcal{J}(\Phi_{\boldsymbol{u}} \boldsymbol{u}_r, \Phi_{\boldsymbol{\mu}} \boldsymbol{\mu}_r)$$

$$\text{subject to} \quad c(\Phi_{\boldsymbol{u}} \boldsymbol{u}_r, \Phi_{\boldsymbol{\mu}} \boldsymbol{\mu}_r) \geq 0$$

$$r(\Phi_{\boldsymbol{u}} \boldsymbol{u}_r, \Phi_{\boldsymbol{\mu}} \boldsymbol{\mu}_r) = 0$$

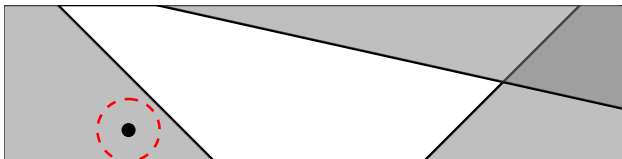
$$\|r(\Phi_{\boldsymbol{u}} \boldsymbol{u}_r, \Phi_{\boldsymbol{\mu}} \boldsymbol{\mu}_r)\| \leq \Delta$$



Elastic constraints to circumvent infeasible subproblems

Constrained Non-Quadratic Trust-Region MOR (CNQTR-MOR)

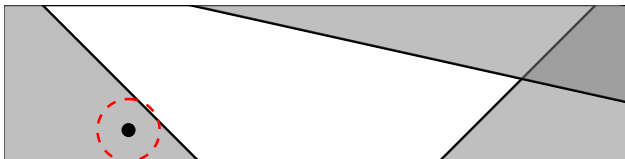
$$\begin{aligned}
& \underset{\mathbf{u}_r \in \mathbb{R}^k \mathbf{u}, \mu_r \in \mathbb{R}^k \boldsymbol{\mu}, \mathbf{t} \in \mathbb{R}^{n_c}}{\text{minimize}} && \mathcal{J}(\Phi_{\mathbf{u}} \mathbf{u}_r, \Phi_{\boldsymbol{\mu}} \boldsymbol{\mu}_r) - \gamma \mathbf{t}^T \mathbf{1} \\
& \text{subject to} && c(\Phi_{\mathbf{u}} \mathbf{u}_r, \Phi_{\boldsymbol{\mu}} \boldsymbol{\mu}_r) \geq \mathbf{t} \\
& && r(\Phi_{\mathbf{u}} \mathbf{u}_r, \Phi_{\boldsymbol{\mu}} \boldsymbol{\mu}_r) = 0 \\
& && \|r(\Phi_{\mathbf{u}} \mathbf{u}_r, \Phi_{\boldsymbol{\mu}} \boldsymbol{\mu}_r)\| \leq \Delta \\
& && \mathbf{t} \leq 0
\end{aligned}$$



Elastic constraints to circumvent infeasible subproblems

Constrained Non-Quadratic Trust-Region MOR (CNQTR-MOR)

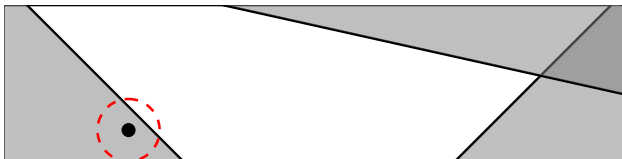
$$\begin{array}{ll}
\text{minimize}_{\mathbf{u}_r \in \mathbb{R}^k \color{red}{u}, \mu_r \in \mathbb{R}^k \color{red}{\mu}, \mathbf{t} \in \mathbb{R}^{n_c}} & \mathcal{J}(\Phi_{\color{red}{u}} \mathbf{u}_r, \Phi_{\color{red}{\mu}} \mu_r) - \gamma \mathbf{t}^T \mathbf{1} \\
\text{subject to} & c(\Phi_{\color{red}{u}} \mathbf{u}_r, \Phi_{\color{red}{\mu}} \mu_r) \geq \mathbf{t} \\
& r(\Phi_{\color{red}{u}} \mathbf{u}_r, \Phi_{\color{red}{\mu}} \mu_r) = 0 \\
& \|r(\Phi_{\color{red}{u}} \mathbf{u}_r, \Phi_{\color{red}{\mu}} \mu_r)\| \leq \Delta \\
& \mathbf{t} \leq 0
\end{array}$$



Elastic constraints to circumvent infeasible subproblems

Constrained Non-Quadratic Trust-Region MOR (CNQTR-MOR)

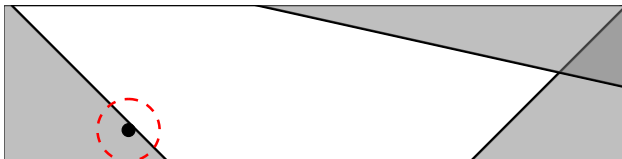
$$\begin{aligned}
& \underset{\mathbf{u}_r \in \mathbb{R}^k \mathbf{u}, \mu_r \in \mathbb{R}^k \boldsymbol{\mu}, \mathbf{t} \in \mathbb{R}^{n_c}}{\text{minimize}} && \mathcal{J}(\Phi_{\mathbf{u}} \mathbf{u}_r, \Phi_{\boldsymbol{\mu}} \boldsymbol{\mu}_r) - \gamma \mathbf{t}^T \mathbf{1} \\
& \text{subject to} && c(\Phi_{\mathbf{u}} \mathbf{u}_r, \Phi_{\boldsymbol{\mu}} \boldsymbol{\mu}_r) \geq \mathbf{t} \\
& && r(\Phi_{\mathbf{u}} \mathbf{u}_r, \Phi_{\boldsymbol{\mu}} \boldsymbol{\mu}_r) = 0 \\
& && \|r(\Phi_{\mathbf{u}} \mathbf{u}_r, \Phi_{\boldsymbol{\mu}} \boldsymbol{\mu}_r)\| \leq \Delta \\
& && \mathbf{t} \leq 0
\end{aligned}$$



Elastic constraints to circumvent infeasible subproblems

Constrained Non-Quadratic Trust-Region MOR (CNQTR-MOR)

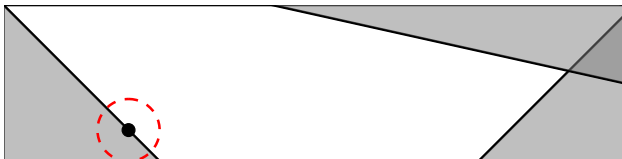
$$\begin{aligned}
& \underset{\mathbf{u}_r \in \mathbb{R}^k \mathbf{u}, \mu_r \in \mathbb{R}^k \boldsymbol{\mu}, \mathbf{t} \in \mathbb{R}^{n_c}}{\text{minimize}} && \mathcal{J}(\Phi_{\mathbf{u}} \mathbf{u}_r, \Phi_{\boldsymbol{\mu}} \boldsymbol{\mu}_r) - \gamma \mathbf{t}^T \mathbf{1} \\
& \text{subject to} && c(\Phi_{\mathbf{u}} \mathbf{u}_r, \Phi_{\boldsymbol{\mu}} \boldsymbol{\mu}_r) \geq \mathbf{t} \\
& && r(\Phi_{\mathbf{u}} \mathbf{u}_r, \Phi_{\boldsymbol{\mu}} \boldsymbol{\mu}_r) = 0 \\
& && \|r(\Phi_{\mathbf{u}} \mathbf{u}_r, \Phi_{\boldsymbol{\mu}} \boldsymbol{\mu}_r)\| \leq \Delta \\
& && \mathbf{t} \leq 0
\end{aligned}$$



Elastic constraints to circumvent infeasible subproblems

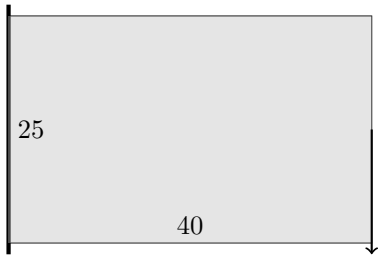
Constrained Non-Quadratic Trust-Region MOR (CNQTR-MOR)

$$\begin{aligned}
& \underset{\mathbf{u}_r \in \mathbb{R}^k \textcolor{red}{u}, \mu_r \in \mathbb{R}^k \textcolor{red}{u}, \mathbf{t} \in \mathbb{R}^{n_c}}{\text{minimize}} && \mathcal{J}(\Phi_{\mathbf{u}} \mathbf{u}_r, \Phi_{\boldsymbol{\mu}} \boldsymbol{\mu}_r) - \gamma \mathbf{t}^T \mathbf{1} \\
& \text{subject to} && c(\Phi_{\mathbf{u}} \mathbf{u}_r, \Phi_{\boldsymbol{\mu}} \boldsymbol{\mu}_r) \geq \mathbf{t} \\
& && r(\Phi_{\mathbf{u}} \mathbf{u}_r, \Phi_{\boldsymbol{\mu}} \boldsymbol{\mu}_r) = 0 \\
& && \|r(\Phi_{\mathbf{u}} \mathbf{u}_r, \Phi_{\boldsymbol{\mu}} \boldsymbol{\mu}_r)\| \leq \Delta \\
& && \mathbf{t} \leq 0
\end{aligned}$$



Compliance Minimization: 2D Cantilever

- 16000 8-node brick elements, 77760 dofs
- Total Lagrangian form, finite strain, StVK⁹
- St. Venant-Kirchhoff material
- Sparse Cholesky linear solver (CHOLMOD¹⁰)
- Newton-Raphson nonlinear solver
- Minimum compliance optimization problem



$$\begin{aligned} & \underset{\boldsymbol{u} \in \mathbb{R}^n u, \boldsymbol{\mu} \in \mathbb{R}^n \mu}{\text{minimize}} && \boldsymbol{f}_{\text{ext}}^T \boldsymbol{u} \\ & \text{subject to} && V(\boldsymbol{\mu}) \leq \frac{1}{2} V_0 \\ & && \boldsymbol{r}(\boldsymbol{u}, \boldsymbol{\mu}) = 0 \end{aligned}$$

- Gradient computations: Adjoint method
- Optimizer: SNOPT [Gill et al., 2002]
- Maximum ROM size: $k_{\boldsymbol{u}} \leq 5$

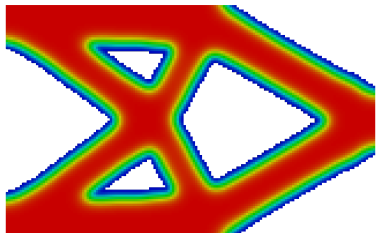


⁹[Bonet and Wood, 1997, Belytschko et al., 2000]

¹⁰[Chen et al., 2008]



Order of Magnitude Speedup to Suboptimal Solution



HDM



CNQTR-MOR + Φ_μ adaptivity

HDM Solution	HDM Gradient	HDM Optimization
7458s (450)	4018s (411)	8284s

HDM

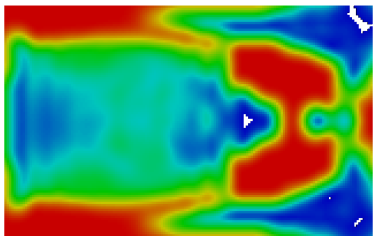
Elapsed time = 19761s

HDM Solution	HDM Gradient	ROB Construction	ROM Optimization
1049s (64)	88s (9)	727s (56)	39s (3676)

CNQTR-MOR + Φ_μ adaptivity
 Elapsed time = 2197s, Speedup $\approx 9x$



Better Solution after 64 HDM Evaluations



HDM

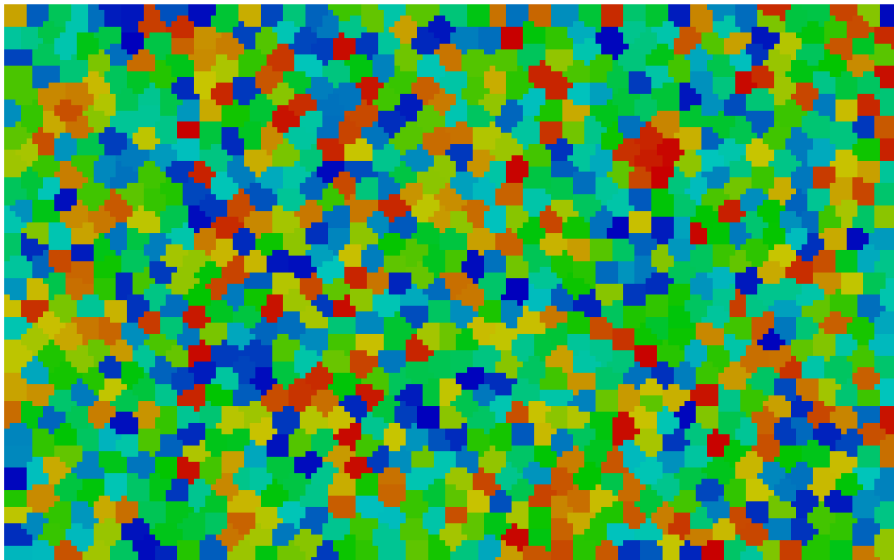


CNQTR-MOR + Φ_μ adaptivity

- CNQTR-MOR + Φ_μ adaptivity: superior approximation to optimal solution than HDM approach after fixed number of HDM solves (64)
- Reasonable option to *warm-start* HDM topology optimization



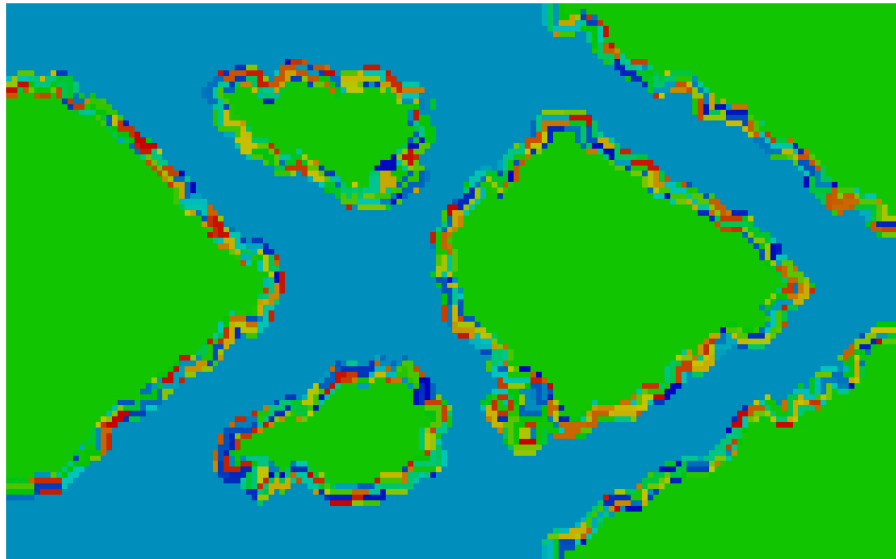
Macro-element Evolution



Iteration 0 (1000)



Macro-element Evolution



Iteration 1 (977)

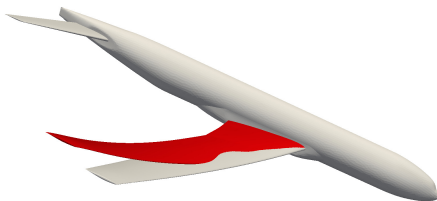


CNQTR-MOR + Φ_μ adaptivity

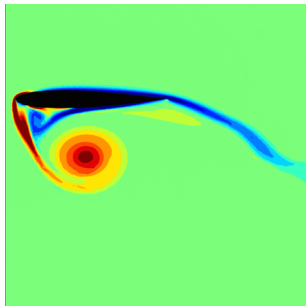


Approaching Many-Query, Extreme-Scale Computational Physics

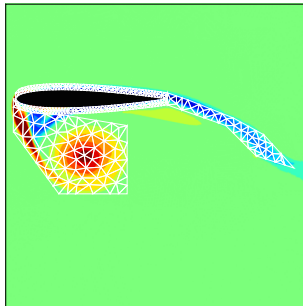
- Framework introduced for accelerating PDE-constrained optimization problem with **side constraints** and **large-dimensional parameter space**
- Speedup attained via adaptive reduction of state space and parameter space
- Concepts borrowed from constrained optimization theory
- Applied to aerodynamic design and topology optimization
 - Order of magnitude speedup observed
 - Competitive warm-start method



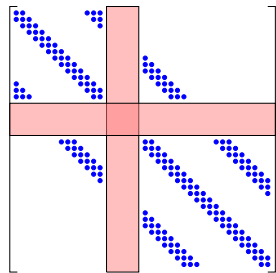
Faster Computational Physics: Adaptive Data-Driven Discretization



(a) Vorticity around heaving airfoil



(b) Potential Ω^l , Ω^g decomposition



(c) Idealized sparsity structure

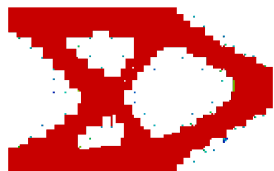
- Methods to *transform* features in global basis functions - minimize reliance on local shape functions
- Linear algebra for sparse operators with a few dense rows and columns
- Integration mesh to mitigate “variational crimes”



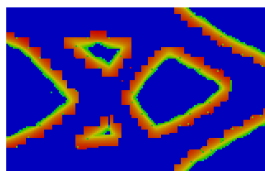
Faster Solvers: Adaptive Reduction of High-Dimensional Optimization

$$\begin{aligned} & \underset{\boldsymbol{\mu}}{\text{minimize}} && f(\boldsymbol{\mu}) \\ & \text{subject to} && c(\boldsymbol{\mu}) = 0 \end{aligned}$$

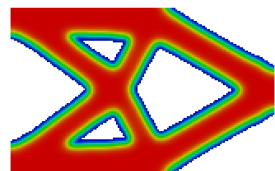
$$\begin{aligned} & \underset{\boldsymbol{\mu}}{\text{minimize}} && f(\Phi_{\boldsymbol{\mu}} \boldsymbol{\mu}_r) \\ & \text{subject to} && c(\Phi_{\boldsymbol{\mu}} \boldsymbol{\mu}_r) = 0 \end{aligned}$$



(a) Sub-optimal sol'n



$$(b) |\nabla_{\mu} \mathcal{L}(\Phi_{\mu} \mu_r, \lambda)|$$



(c) Optimal solution

- Prove global convergence and develop into general, constrained optimizer
 - Further develop into topology optimization solver - *overcome checkerboard*



Fewer Queries: Second-Order Methods for Accelerated Convergence

Hessian information highly desired in optimization and UQ, but expensive due to $\mathcal{O}(N_{\mu})$ required linear system solves

Sensitivity/Adjoint Method for Computing Hessian

$$\begin{aligned} \frac{d^2 \mathcal{J}}{d\boldsymbol{\mu}_j d\boldsymbol{\mu}_k} &= \frac{\partial^2 \mathcal{J}}{\partial \boldsymbol{\mu}_j \partial \boldsymbol{\mu}_k} + \frac{\partial^2 \mathcal{J}}{\partial \boldsymbol{\mu}_j \partial \boldsymbol{u}} \frac{\partial \boldsymbol{u}}{\partial \boldsymbol{\mu}_k} + \frac{\partial \boldsymbol{u}}{\partial \boldsymbol{\mu}_j}^T \frac{\partial^2 \mathcal{J}}{\partial \boldsymbol{u} \partial \boldsymbol{\mu}_k} + \frac{\partial \boldsymbol{u}}{\partial \boldsymbol{\mu}_j}^T \frac{\partial^2 \mathcal{J}}{\partial \boldsymbol{u} \partial \boldsymbol{u}} \frac{\partial \boldsymbol{u}}{\partial \boldsymbol{\mu}_k} \\ &\quad - \frac{\partial \mathcal{J}}{\partial \boldsymbol{u}} \frac{\partial \boldsymbol{r}}{\partial \boldsymbol{u}}^{-1} \left[\frac{\partial^2 \boldsymbol{r}}{\partial \boldsymbol{\mu}_j \partial \boldsymbol{\mu}_k} + \frac{\partial^2 \boldsymbol{r}}{\partial \boldsymbol{\mu}_j \partial \boldsymbol{u}} \frac{\partial \boldsymbol{u}}{\partial \boldsymbol{\mu}_k} + \frac{\partial^2 \boldsymbol{r}}{\partial \boldsymbol{\mu}_k \partial \boldsymbol{u}} \frac{\partial \boldsymbol{u}}{\partial \boldsymbol{\mu}_j} + \frac{\partial^2 \boldsymbol{r}}{\partial \boldsymbol{u} \partial \boldsymbol{u}} : \frac{\partial \boldsymbol{u}}{\partial \boldsymbol{\mu}_j} \otimes \frac{\partial \boldsymbol{u}}{\partial \boldsymbol{\mu}_k} \right] \end{aligned}$$

where

$$\frac{\partial \boldsymbol{u}}{\partial \boldsymbol{\mu}_j} = \frac{\partial \boldsymbol{r}}{\partial \boldsymbol{u}}^{-1} \frac{\partial \boldsymbol{r}}{\partial \boldsymbol{\mu}_j}$$

- Fast, *multiple right-hand side* linear solver by building data-driven subspace for image of $\frac{\partial \boldsymbol{r}}{\partial \boldsymbol{u}}, \frac{\partial \boldsymbol{r}}{\partial \boldsymbol{u}}^{-T}$
- Similar to Krylov methods that use *a-priori, analytical* subspace



Acknowledgement



References I

-  Barbic, J. and James, D. (2007).
Time-critical distributed contact for 6-dof haptic rendering of adaptively sampled reduced deformable models.
In *Proceedings of the 2007 ACM SIGGRAPH/Eurographics symposium on Computer animation*, pages 171–180. Eurographics Association.
-  Barrault, M., Maday, Y., Nguyen, N. C., and Patera, A. T. (2004).
An empirical interpolation method: application to efficient reduced-basis discretization of partial differential equations.
Comptes Rendus Mathematique, 339(9):667–672.
-  Belytschko, T., Liu, W., Moran, B., et al. (2000).
Nonlinear finite elements for continua and structures, volume 26.
Wiley New York.
-  Bonet, J. and Wood, R. (1997).
Nonlinear continuum mechanics for finite element analysis.
Cambridge university press.
-  Bui-Thanh, T., Willcox, K., and Ghattas, O. (2008).
Model reduction for large-scale systems with high-dimensional parametric input space
SIAM Journal on Scientific Computing, 30(6):3270–3288.



References II

-  Carlberg, K., Bou-Mosleh, C., and Farhat, C. (2011).
Efficient non-linear model reduction via a least-squares petrov–galerkin projection and compressive tensor approximations.
International Journal for Numerical Methods in Engineering, 86(2):155–181.
-  Chapman, T., Collins, P., Avery, P., and Farhat, C. (2015).
Accelerated mesh sampling for model hyper reduction.
International Journal for Numerical Methods in Engineering.
-  Chaturantabut, S. and Sorensen, D. C. (2010).
Nonlinear model reduction via discrete empirical interpolation.
SIAM Journal on Scientific Computing, 32(5):2737–2764.
-  Chen, Y., Davis, T. A., Hager, W. W., and Rajamanickam, S. (2008).
Algorithm 887: Cholmod, supernodal sparse cholesky factorization and update/downdate.
ACM Transactions on Mathematical Software (TOMS), 35(3):22.
-  Constantine, P. G., Dow, E., and Wang, Q. (2014).
Active subspace methods in theory and practice: Applications to kriging surfaces.
SIAM Journal on Scientific Computing, 36(4):A1500–A1524.



References III

-  Fahl, M. (2001).
Trust-region methods for flow control based on reduced order modelling.
PhD thesis, Universitätsbibliothek.
-  Gill, P. E., Murray, W., and Saunders, M. A. (2002).
Snopt: An sqp algorithm for large-scale constrained optimization.
SIAM journal on optimization, 12(4):979–1006.
-  Lawson, C. L. and Hanson, R. J. (1974).
Solving least squares problems, volume 161.
SIAM.
-  Lieberman, C., Willcox, K., and Ghattas, O. (2010).
Parameter and state model reduction for large-scale statistical inverse problems.
SIAM Journal on Scientific Computing, 32(5):2523–2542.
-  Maute, K. and Ramm, E. (1995).
Adaptive topology optimization.
Structural optimization, 10(2):100–112.



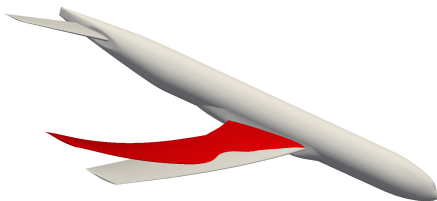
References IV

-  Nguyen, N. and Peraire, J. (2008).
An efficient reduced-order modeling approach for non-linear parametrized partial differential equations.
International journal for numerical methods in engineering, 76(1):27–55.
-  Nocedal, J. and Wright, S. (2006).
Numerical optimization, series in operations research and financial engineering.
Springer.
-  Rewienski, M. J. (2003).
A trajectory piecewise-linear approach to model order reduction of nonlinear dynamical systems.
PhD thesis, Citeseer.
-  Zahr, M. J. and Farhat, C. (2014).
Progressive construction of a parametric reduced-order model for pde-constrained optimization.
International Journal for Numerical Methods in Engineering.

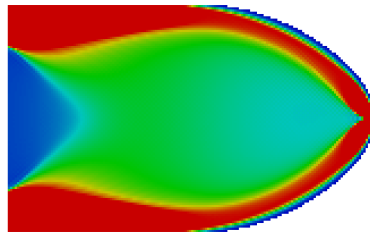


Approaching Many-Query, Extreme-Scale Computational Physics

- Framework introduced for accelerating PDE-constrained optimization problem with **side constraints** and **large-dimensional parameter space**
- Speedup attained via adaptive reduction of state space and parameter space
- Concepts borrowed from constrained optimization theory
- Applied to aerodynamic design and topology optimization
 - Order of magnitude speedup observed
 - Competitive warm-start method



Standard Difficulty: Binary Solutions



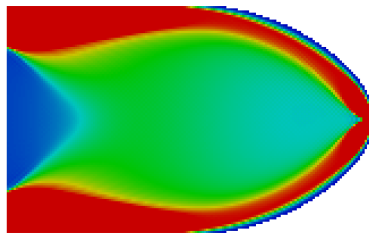
(a) Without penalization



Standard Difficulty: Binary Solutions

Relaxed, Penalized Problem Setup

$$\begin{aligned} & \underset{\boldsymbol{u} \in \mathbb{R}^{n_u}, \boldsymbol{\mu} \in \mathbb{R}^{n_\mu}}{\text{minimize}} \quad \boldsymbol{f}_{\text{ext}}^T \boldsymbol{u} \\ & \text{subject to} \quad V(\boldsymbol{\mu}) \leq \frac{1}{2} V_0 \\ & \quad \mathbf{r}(\boldsymbol{u}, \boldsymbol{\mu}^p) = 0 \\ & \quad \boldsymbol{\mu} \in [0, 1]^k \end{aligned}$$



(a) Without penalization

Effect of Penalization

$$\mathbf{K}^e \leftarrow (\mu^e)^p \mathbf{K}^e$$

- \mathbf{K}^e : eth element stiffness matrix



Standard Difficulty: Binary Solutions

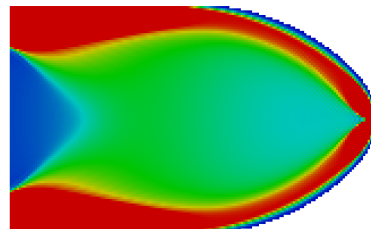
Relaxed, Penalized Problem Setup

$$\underset{\boldsymbol{u} \in \mathbb{R}^{n_{\boldsymbol{u}}}, \boldsymbol{\mu} \in \mathbb{R}^{n_{\boldsymbol{\mu}}}}{\text{minimize}} \quad \boldsymbol{f}_{\text{ext}}^T \boldsymbol{u}$$

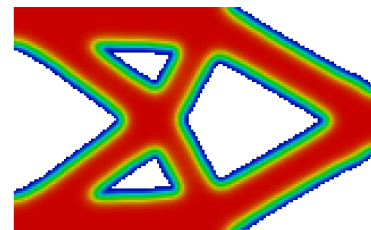
$$\text{subject to} \quad V(\boldsymbol{\mu}) \leq \frac{1}{2} V_0$$

$$\mathbf{r}(\boldsymbol{u}, \boldsymbol{\mu}^p) = 0$$

$$\boldsymbol{\mu} \in [0, 1]^{k_{\boldsymbol{\mu}}}$$



(a) Without penalization



(b) With penalization

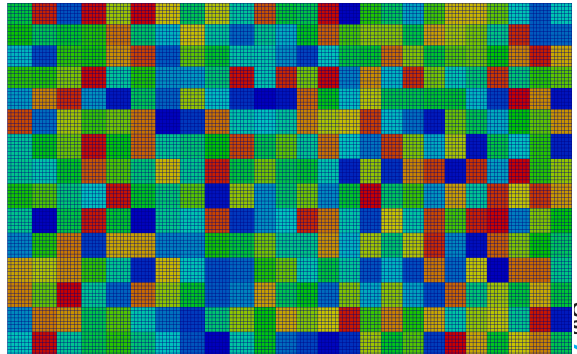
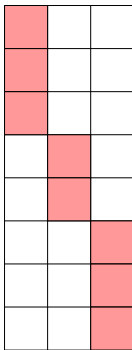


• $\mathbf{K}^e \leftarrow (\boldsymbol{\mu}^e)^p \mathbf{K}^e$

Standard Difficulty: Binary Solutions

Implication for ROM

- From parameter restriction, $\mu^p = (\Phi_\mu \mu_r)^p$
- Precomputation relies on separability of Φ_μ and μ_r
- Separability maintained if $(\Phi_\mu \mu_r)^p = \Phi_\mu \mu_r^p$
- Sufficient condition: *columns of Φ_μ have non-overlapping non-zeros*



Efficient Evaluation of Nonlinear Terms

- Due to the mixing of high-dimensional and low-dimensional terms in the ROM expression, only limited speedups available

$$\mathbf{r}_r(\boldsymbol{u}_r, \boldsymbol{\mu}_r) = \Phi_{\boldsymbol{u}}^T \mathbf{r}(\Phi_{\boldsymbol{u}} \boldsymbol{u}_r, \Phi_{\boldsymbol{\mu}} \boldsymbol{\mu}_r) = 0$$

- To enable *pre-computation* of all large-dimensional quantities into low-dimensional ones, leverage *Taylor series expansion*

$$[\mathbf{r}_r(\boldsymbol{u}_r, \boldsymbol{\mu}_r)]_i = \mathbf{D}_{im}^0(\boldsymbol{\mu}_r)_m + \mathbf{D}_{ijm}^1(\boldsymbol{u}_r \times \boldsymbol{\mu}_r)_{jm} + \mathbf{D}_{ijkm}^2(\boldsymbol{u}_r \times \boldsymbol{u}_r \times \boldsymbol{\mu}_r)_{jkm} \\ + \mathbf{D}_{ijklm}^3(\boldsymbol{u}_r \times \boldsymbol{u}_r \times \boldsymbol{u}_r \times \boldsymbol{\mu}_r)_{jklm} = 0$$

where

$$\mathbf{D}_{ijklm}^3 = \frac{\partial^3 \mathbf{r}_t}{\partial \boldsymbol{u}_p \partial \boldsymbol{u}_q \partial \boldsymbol{u}_s}(\hat{\boldsymbol{u}}, \boldsymbol{\phi}_{\boldsymbol{\mu}}^m)(\boldsymbol{\phi}_{\boldsymbol{u}}^i \times \boldsymbol{\phi}_{\boldsymbol{u}}^j \times \boldsymbol{\phi}_{\boldsymbol{u}}^k \times \boldsymbol{\phi}_{\boldsymbol{u}}^l)_{tpqs}$$

- Related work: [Rewienski, 2003, Barrault et al., 2004, Barbić and James, 2007, Nguyen and Peraire, 2008, Chaturantabut and Sorensen, 2010, Carlberg et al., 2011]



Lagrange Multiplier Estimate

Lagrange Multiplier, Constraint Pairs

λ	λ_r	τ	τ_r
$\mathbf{c}(\mathbf{u}, \boldsymbol{\mu}) \geq 0$	$\mathbf{c}(\Phi_{\mathbf{u}} \mathbf{u}_r, \Phi_{\boldsymbol{\mu}} \boldsymbol{\mu}) \geq 0$	$\mathbf{A} \boldsymbol{\mu} \geq \mathbf{b}$	$\mathbf{A}_r \boldsymbol{\mu}_r \geq \mathbf{b}_r$

Goal: Given $\mathbf{u}_r, \boldsymbol{\mu}_r, \tau_r \geq 0, \lambda_r \geq 0$, estimate $\tilde{\tau} \geq 0, \tilde{\lambda} \geq 0$ to compute

$$\nabla_{\boldsymbol{\mu}} \mathcal{L}(\Phi_{\boldsymbol{\mu}} \boldsymbol{\mu}_r, \tilde{\lambda}, \tilde{\tau}) = \frac{\partial \mathcal{J}}{\partial \boldsymbol{\mu}}(\Phi_{\mathbf{u}} \mathbf{u}_r, \Phi_{\boldsymbol{\mu}} \boldsymbol{\mu}_r) - \frac{\partial \mathbf{c}}{\partial \boldsymbol{\mu}}(\Phi_{\mathbf{u}} \mathbf{u}_r, \Phi_{\boldsymbol{\mu}} \boldsymbol{\mu}_r)^T \tilde{\lambda} - \mathbf{A}^T \tilde{\tau}$$

Lagrange Multiplier Estimates

$$\tilde{\lambda} = \lambda_r$$

$$\tilde{\tau} = \arg \min_{\tau \geq 0} \left\| \mathbf{A}^T \tau - \left(\frac{\partial \mathcal{J}}{\partial \boldsymbol{\mu}}(\Phi_{\mathbf{u}} \mathbf{u}_r, \Phi_{\boldsymbol{\mu}} \boldsymbol{\mu}_r) - \frac{\partial \mathbf{c}}{\partial \boldsymbol{\mu}}(\Phi_{\mathbf{u}} \mathbf{u}_r, \Phi_{\boldsymbol{\mu}} \boldsymbol{\mu}_r)^T \tilde{\lambda} \right) \right\|$$



Non-negative least squares: [Lawson and Hanson, 1974, Chapman et al., 2015]



Standard Difficulty: Checkerboarding

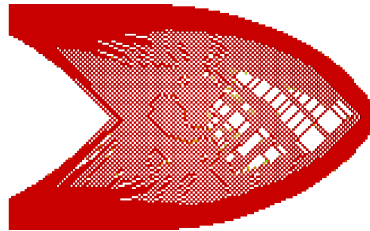
Gradient Filtering, Nodal Projection

- Minimum length scale, r_{\min}
- Gradient Filtering¹¹

$$\frac{\widehat{\partial \mathcal{J}}}{\partial \boldsymbol{\mu}_k} = \frac{\sum_{j \in S_k} H_{kj} \boldsymbol{\mu}_i \frac{\partial \mathcal{J}}{\partial \boldsymbol{\mu}_i}}{\boldsymbol{\mu}_k \sum_{j \in S_k} H_{kj}}$$

- Nodal Projection

$$\boldsymbol{\mu}_k = \frac{\sum_{j \in \mathcal{S}_k} \boldsymbol{\tau}_j H_{jk}}{\sum_{j \in \mathcal{S}_k} H_{jk}}$$



(a) Without projection/filtering



¹¹ $H_{ki} = r_{\min} - \text{dist}(k, i)$

Standard Difficulty: Checkerboarding

Gradient Filtering, Nodal Projection

- Minimum length scale, r_{\min}
- Gradient Filtering¹¹

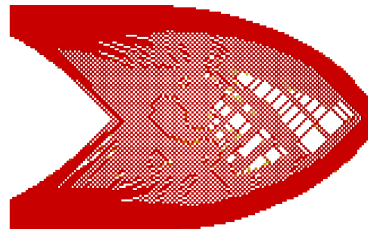
$$\widehat{\frac{\partial \mathcal{J}}{\partial \boldsymbol{\mu}_k}} = \frac{\sum_{j \in S_k} H_{kj} \boldsymbol{\mu}_i \frac{\partial \mathcal{J}}{\partial \boldsymbol{\mu}_i}}{\boldsymbol{\mu}_k \sum_{j \in S_k} H_{kj}}$$

- Nodal Projection

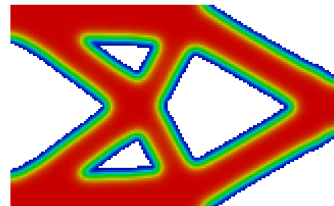
$$\boldsymbol{\mu}_k = \frac{\sum_{j \in \mathcal{S}_k} \tau_j H_{jk}}{\sum_{j \in \mathcal{S}_k} H_{jk}}$$



¹¹ $H_{ki} = r_{\min} - \text{dist}(k, i)$

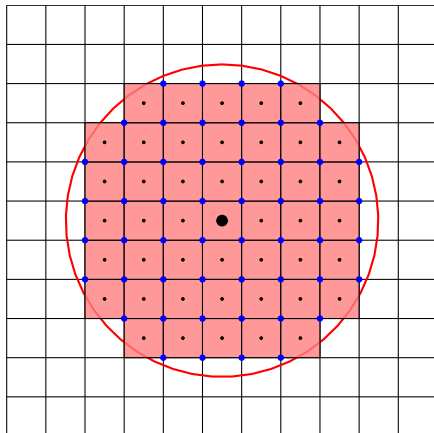


(a) Without projection/filtering

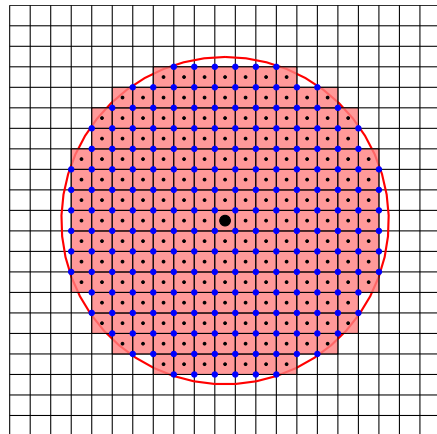


(b) With projection

Standard Difficulty: Checkerboarding



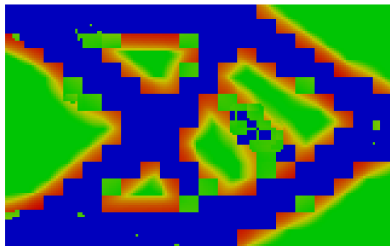
Standard Difficulty: Checkerboarding



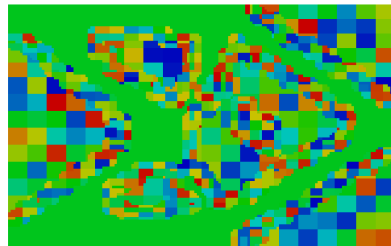
Standard Difficulty: Checkerboarding

Implication for ROM

- Nonlocality introduced through projection/filtering
- μ_e influences volume fraction of all elements within r_{\min} of element/node e
- Clashes with requirement on Φ_μ of columns with non-overlapping non-zeros
- Handled heuristically by performing parameter basis adaptation to eliminate “checkerboard” regions of parameter space, uses concept of r_{\min}
- *Next: Helmholtz filtering*



Gradient of Lagrangian



Updated Macroelements

